

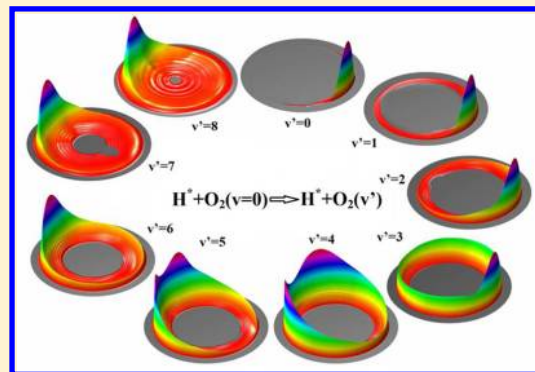
Observation of Extremely High Vibrational Excitation in O₂ from Inelastic Scattering of Rydberg H Atom with O₂

Shengrui Yu, Shu Su, Kaijun Yuan,* Dongxu Dai, and Xueming Yang*

State Key Laboratory of Molecular Reaction Dynamics, Dalian Institute of Chemical Physics, Chinese Academy of Sciences, 457 Zhongshan Road Dalian 116023, China

ABSTRACT: The state-resolved differential cross sections for the Rydberg-atom (RA) inelastic scattering process $H^*(n = 46) + O_2(v = 0, j = 1, 3) \rightarrow H^*(n') + O_2(v', j')$ have been measured by using the H-atom Rydberg tagging time-of-flight (HRTOF) technique. Extensive vibrational excitation of O₂ products has been observed at the two collision energies of 0.64 and 1.55 eV. Experimental results show that the O₂ products in the low vibrationally excited states are clearly forward-scattered, whereas those in the highly vibrationally excited states are mainly backward-scattered. Partially resolved rotational structures were also observed and assigned. The striking observation of extremely high energy transfer from translational to vibrational excitation at the backward direction could be explained involving charge transfer between proton and O₂ molecule and possibly complex formation during the scattering process.

SECTION: Spectroscopy, Photochemistry, and Excited States



Inelastic collisions are a fundamental collision process in which some of the kinetic energy of the colliding partner transfers to vibrational or rotational energy. A detailed understanding of the nature and outcome of the inelastic collision plays an important role in atmospheric chemistry, combustion chemistry, and interstellar chemistry. It also could provide a sensitive test for molecular interaction potentials and the formation mechanism of a short-lived reactive collision complex. In the past few decades, dozens of experimental and theoretical studies have been performed on atom–molecule and proton–molecule inelastic collisions.^{1–4}

Atom–molecule inelastic scattering is usually treated by involving the repulsive part of the potential, and it is assumed to happen by means of impulsive compression of one of the bonds of the collision partners. This behavior has been proven to be successful in interpreting the results for the vibrational excitation of molecular targets in some collision systems, such as He + H₂,⁴ H + CO,^{5,6} and H + CO₂,⁷ whereas sometimes attractive forces between the collision partners also play a role in the vibrational energy-transfer process.⁸ More recently, Zare and coworkers^{9,10} observed the anomalous behavior for the simplest inelastic scattering process H + o-D₂, in which the vibrationally excited products are dominantly forward-scattered. They suggested a new mechanism for vibrational excitation that should play a role in all neutral–neutral collisions where strong attraction can develop between the collision partners.

Proton–molecule inelastic collisions have also attracted much attention in the past few years. The scattering of protons with N₂ and CO at $E_{\text{cm}} = 12$ eV was first investigated experimentally by Udseth et al.,¹¹ but their energy resolution was too low to resolve the individual vibrational transition. Vibrationally resolved scattering of H⁺ with N₂, CO, and NO at

higher energies in the range of $E_{\text{Lab}} = 30\text{--}80$ eV has recently been reported by Krutein and Linder.¹² They found a relatively low vibrational energy transfer in the processes of the collisions. In contrast, the H⁺–O₂ system exhibits a very strong vibrational inelasticity.^{13–16} An explanation was proposed in terms of an intermediate charge-transfer mechanism involving the crossing of the O₂(³Σ_g[−]) + H⁺ and O₂⁺(²Π_g) + H potential surfaces. Although a vast amount of data is available from inelastic scattering of proton–molecule collision, the most detailed information involving rotational and vibrational distributions is still not well understood. The main reason is that there is a serious problem for the ion–molecule scattering, in which the trajectories of ion products could be affected by the electric field applied to control the ion beam. This problem is especially serious for low-energy ion products and severely limits experimental resolution of the time-of-flight for ion products. The inelastic collisions with neutral high-*n* Rydberg-atom (RA), however, do not suffer this problem.

Recently, the dynamics of RA reactive scattering $H^*(n) + D_2 \rightarrow HD + D^*(n')$ have been closely investigated.^{17–19} It was found that the rotationally resolved product distribution for the RA reaction was in a good agreement with that obtained at a single scattering angle for the proton–diatom reaction $H^+ + D_2 \rightarrow HD + D^+$.²⁰ These results are consistent with the Fermi independent-collider model,^{21–23} wherein the Rydberg electron of the highly excited RA effectively behaves as a spectator. A similar conclusion has also been obtained in RA inelastic

Received: July 24, 2012

Accepted: August 15, 2012

scattering previously studied by Davis and coworkers.²⁴ They presented vibrationally resolved inelastic scattering of H-RA from N₂ and O₂ at the collision energy of 1.84 eV. Up to $\nu = 4$ of O₂ products are observed from the inelastic process of H-RA with O₂ at the collision energy of 1.84 eV. However, recent studies by Yu et al. cautioned that ionic core and Rydberg electron coupling cannot be neglected in the DCSs of H* + D₂ reactive scattering.²⁵ This encourages us to examine further the inelastic scattering dynamics of the H-RA with other molecules to see if ionic core and Rydberg electron coupling is important. Here we would like to present the state-resolved DCSs for inelastic scattering of H-RA with O₂.

In the current work, we have reinvestigated the typical inelastic collision of H-RA with O₂ at two lower collision energies of 0.64 and 1.55 eV by using the H-atom Rydberg tagging time-of-flight (HRTOF) technique, which has been applied to the study of the collision dynamics of H* + *o*-D₂.^{17,25} TOF spectra of the scattered H-RA products from the H* ($n = 46$) + O₂ → H*(n') + O₂ collision at 17 laboratory scattering angles (from 85 to -70° at a $\sim 10^\circ$ interval) have been measured. The direction of the O₂ beam is $\theta_{\text{Lab}} = 0^\circ$, whereas the direction of the H-RA beam is $\theta_{\text{Lab}} = 90^\circ$. Those TOF spectra can be converted to the velocity spectra using a standard Jacobian transformation. Figure 1 illustrates two

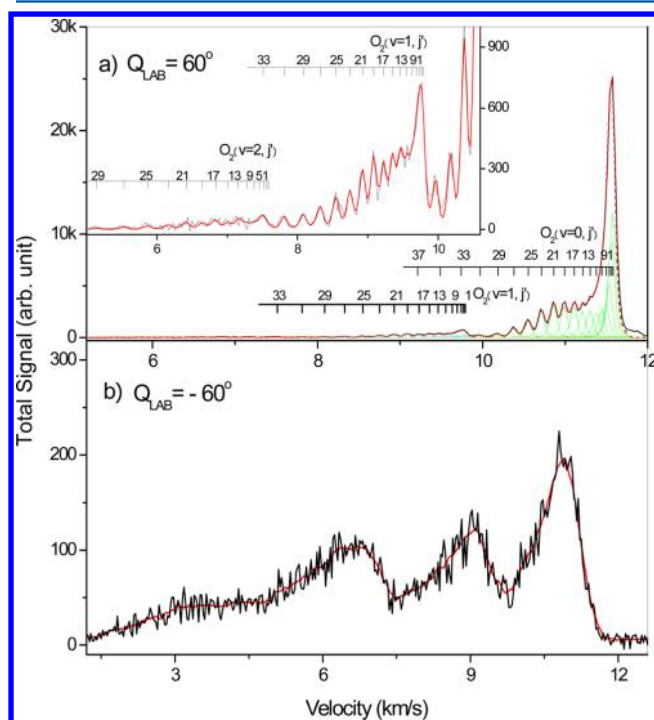


Figure 1. Velocity spectra of the scattered Rydberg H atoms from the H* ($n = 46$) + O₂ → H*(n') + O₂ collision at the collision energy of 0.64 eV: (a) $\theta_{\text{Lab}} = 60^\circ$ (forward scattering, the same direction as the initial direction of each collision partner); (b) $\theta_{\text{Lab}} = -60^\circ$ (backward scattering). The observed peaks are simulated by the individual profiles corresponding to the different O₂ rotational states.

typical velocity spectra at the collision energy of 0.64 eV, which correspond to the scattering products roughly in the forward ($\theta_{\text{Lab}} = 60^\circ$) and backward ($\theta_{\text{Lab}} = -60^\circ$) directions in the center-of-mass (CM) frame. A series of broad peaks have been observed in Figure 1, which can be assigned to the different vibrational excited states of the O₂ products. It is interesting

that rotational distributions are partially resolved in the forward direction. Because the nuclear spin quantum number of the O¹⁶ isotope is zero, only the one symmetry modification with odd-numbered rotational states does exist for the homonuclear O₂ molecule. All of the individual peaks in Figure 1a could be clearly assigned to the odd- j' rotational levels with different vibrational excitation. This phenomenon has also been observed in the process of Ar + O₂ collisions.²⁷ In the backward direction, vibrationally inelastic scattering becomes more prominent. Note that O₂ product peaks out to $\nu = 3$ are seen in Figure 1b.

Figure 2 shows two velocity spectra at the collision energy of 1.55 eV, which also correspond to the scattering products in the

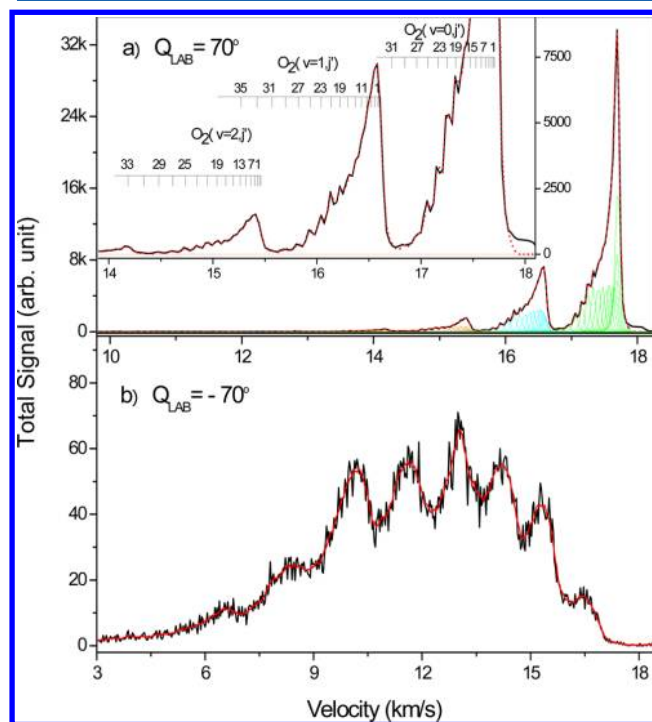


Figure 2. Velocity spectra of the scattered Rydberg H atoms from the H* ($n = 46$) + O₂ → H*(n') + O₂ collision at the collision energy of 1.55 eV: (a) $\theta_{\text{Lab}} = 70^\circ$ (forward scattering); (b) $\theta_{\text{Lab}} = -70^\circ$ (backward scattering). The observed peaks are simulated by the individual profiles corresponding to the different O₂ rotational states.

forward and backward directions in the CM frame. The rotational distributions are also partially resolved in the forward direction but more ambiguous than those in the 0.64 eV collision. Pronounced vibrational excitation has also been observed in the backward direction at the collision energy of 1.55 eV. One marked difference from that in the 0.64 eV collision is the populations of vibrationally excited O₂ products with $\nu = 1-6$ are more intense than that with $\nu = 0$.

Those velocity spectra obtained experimentally in the laboratory frame are simulated by adjusting the relative populations of the rovibrational states of the O₂ products. From these fits, relative populations of O₂ products at different rovibrational states were determined at 17 LAB angles. State-resolved distributions of the O₂ products in the CM frame were then determined by a polynomial fit to the above results, and from these distributions, state-resolved DCSs were determined. By incorporating all of the velocity distribution in the CM frame, a 3D contour plot of the DCSs for the total H-RA

products and for H-RA products corresponding to each individual O_2 vibrational state is shown in Figure 3. It is

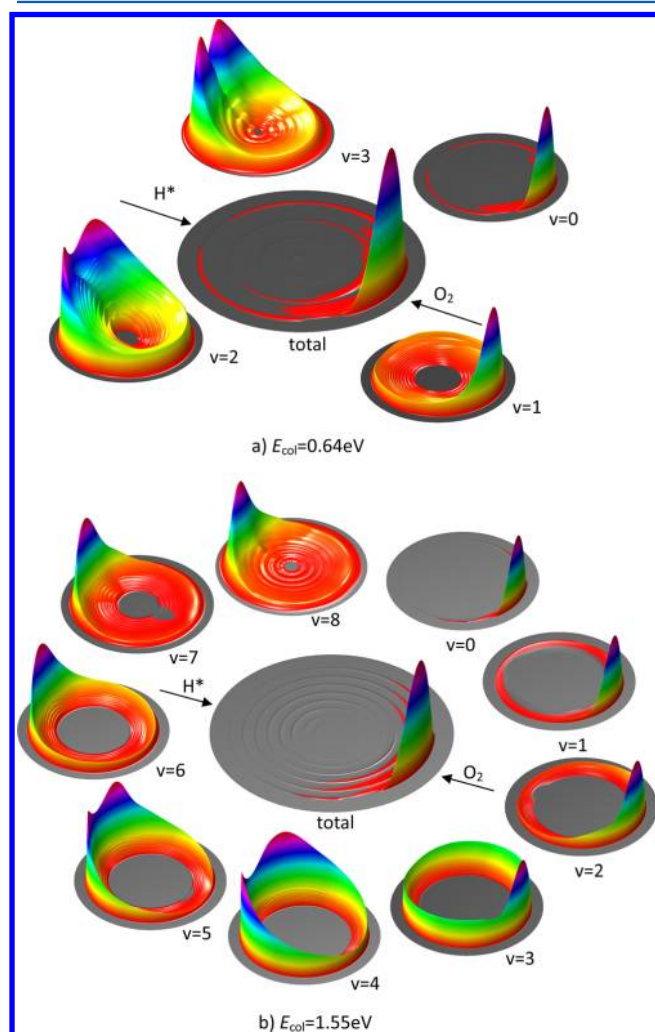


Figure 3. Three-dimensional product contour plots for the total H-RA products and the H-RA products corresponding to the O_2 product from $v = 0$ to 3 with the collision energy of 0.64 eV (a) and $v = 0$ to 8 with the collision energy of 1.55 eV (b). Different layer structures correspond to the O_2 rotational structures in each individual v plot. The energetic limit for each plot is different. The H-RA beam direction is the forward scattering direction.

found that state-resolved DCSs change dramatically with different vibrationally excited states. The angular distributions for the O_2 products at all different vibrational states were determined by integrating over all of the rotational-state populations for each vibrational level. Figure 4a shows such angular distributions for the O_2 products at $v = 0$ to 3 at the collision energy of 0.64 eV. For O_2 ($v = 0$) products, the DCS presents forward scattering, and the DCS for O_2 ($v = 1$) products is still forward-scattered with some extent of sideways-scattered, whereas for O_2 ($v = 2, 3$) products, the DCSs become nearly backward-scattered. This change is much more significant at the collision energy of 1.55 eV. As shown in Figures 3b and 4b, the relatively intensive peak of the angular distributions appears near 0° for O_2 products at $v = 0-2$, then changes to $\sim 60^\circ$ for O_2 products at $v = 3$ and $\sim 140^\circ$ for O_2 products at $v = 4$, with a final change to near 180° for O_2 products at $v = 6-8$.

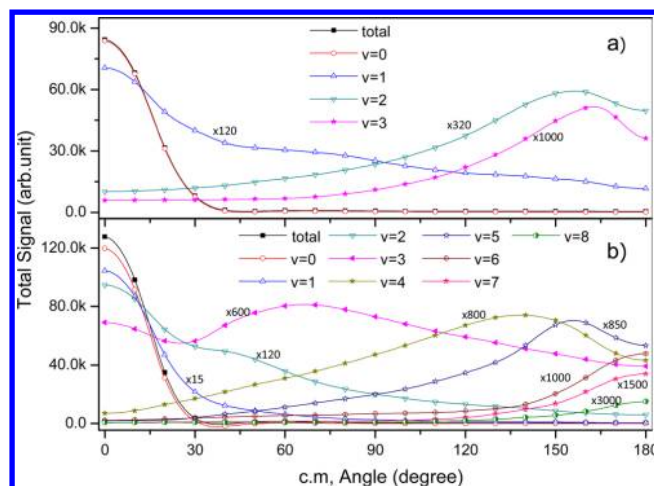


Figure 4. State-resolved experimental differential cross sections for the vibrational excitation of O_2 products from the $H^*(n = 46) + O_2$ inelastic scattering at two different collision energies: (a) $E_{\text{col}} = 0.64 \text{ eV}$ and (b) $E_{\text{col}} = 1.55 \text{ eV}$.

The conventional wisdom for inelastic collision is that collisions with high-impact parameters are forward-scattered and essentially low-energy transfer from kinetic energy to vibrational energy, whereas collisions with low-impact parameters transfer a large amount of energy into vibrations and are mainly backward-scattered. The state-resolved DCSs observed in this work are exactly consistent with such propensity. This is quite different from vibrationally inelastic $H + D_2$ collisions studied by Zare and coworkers,^{9,10} in which they observed that the D_2 products are dominantly forward-scattered at all vibrational excited states and attributed such phenomenon to strong attractive forces when H atom grazes D_2 molecule. Anomalous forward scattering in vibrational inelastic collision has also been observed previously in ion–molecule reactions. A particularly notable example was the demonstration that forward scattering in vibrationally inelastic scattering of H^+ with H_2 , HD, and D_2 reported by Giese et al.²⁶ They suggested a different mechanism in which the passing proton withdraws electron density from the diatomic target, stretches the bond of target molecule, and induces vibrational excitation. As for our case, the mechanism for vibrationally inelastic scattering is different. There is a well-defined crossing between the $O_2(^3\Sigma_g^-) + H^+$ and $O_2(^2\Pi_g) + H$ potential surfaces at 3 Å. At large impact parameters ($>3 \text{ Å}$) charge transfer cannot occur, so vibrational excitation in the forward direction is not efficient. Whereas at small impact parameters ($<3 \text{ Å}$), charge transfer could happen between proton and O_2 . Because the equilibrium bond length of O_2^+ is considerably smaller than in O_2 , substantial vibrational excitation could be observed in the backward direction.

Total quantum state distributions for inelastic scattering of H-RA with O_2 can be determined by integrating those DCSs over different CM angles. The O_2 rotational state distributions at each vibrational level are displayed in Figure 5. For comparison, rotational state distributions for different vibrational level have different scales. From those distributions, it is quite clear that all of the rotational distributions are close to Boltzmann distributions at both collision energies. The O_2 ($v = 0, j' = 1$) products with strong intensity for both collision energies obviously come from the elastic scattering. For collision energy of 0.64 eV, the relative population of rotational

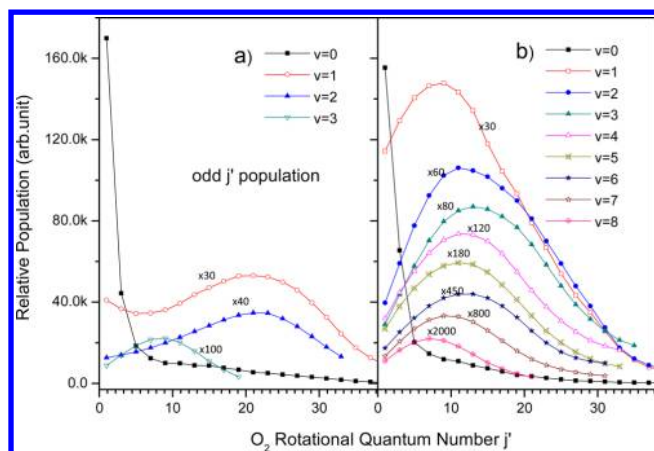


Figure 5. Rotational distributions of the O_2 products at different vibrational states for the $H^*(n=46) + O_2$ scattering at two different collision energies: (a) $E_{col} = 0.64$ eV and (b) $E_{col} = 1.55$ eV.

states of O_2 products at the vibrational ground state decreases dramatically as the rotational energy increases. However, the rotational distributions for vibrational excited $O_2(v=1, 2)$ products are a little hot with the intensive peak of $j' = 21$, whereas the rotational distribution for vibrational excited $O_2(v=3)$ products is moderate with the intensive peak of $j' = 9$. For collision energy of 1.55 eV, all of the rotational distributions are a little colder. It seems that the rotational excitation is relatively smaller at higher collision energy.

The most striking phenomenon observed in this work is the extremely high vibrational excitation of O_2 products in the backward-scattered direction. At the collision energy of 0.64 eV, the O_2 products at $v=3$ have been observed, which means that $\sim 89\%$ kinetic energy transfers to vibrational energy, whereas for collision energy of 1.55 eV, O_2 peaks out to $v=7$ are clearly seen (Figure 2b). That means $\sim 83\%$ kinetic energy transfers to the $O_2(v=7)$ products, and even more than 90% kinetic energy transfers to the $O_2(v=8)$ products. This is interesting because translational to vibrational energy transfer in atom–molecule or ion–molecule collisions is generally inefficient. Similar anomalous vibrational excitation was also seen in the collision of H^+ with O_2 at $E_{col} = 9.8$ eV by Gianturco et al.¹³ and in the collision of H-RA with O_2 at $E_{col} = 1.84$ eV by Strazisar et al.²⁴ They attributed this phenomenon to a temporary intermediate charge transfer between H^+ and O_2 , which can only occur at internuclear distances of 3 Å. In the transition to $H + O_2^+$ surface and back to $H^+ + O_2$ surface, strong impulsive forces are exerted on the molecular bond, which leads to a particularly large vibrational excitation. This work, however, is the first to observe near 90% of kinetic energy transfer in the vibrationally inelastic scattering in the backward-scattered direction. The possible reason is the short-lived H–O–O complex formation could occur when H-RA nearly collinearly collides with O_2 . Detailed theoretical investigations are still needed to understand this phenomenon.

From the above study, the state-to-state dynamics of H-RA scattering with O_2 have been investigated using the HRTOF method. State-resolved DCSs were obtained at two collision energies of 0.64 and 1.55 eV. Up to $v=8$ of O_2 scattering products were observed from the scattering of H-RA with $O_2(v=0)$ at 1.55 eV. Experimental results show that the DCSs of different vibrational levels change dramatically. The trend of angular distribution variation seems to be consistent with the

conventional wisdom of inelastic collision. A charge-transfer mechanism for O_2 could be responsible for such phenomenon. The existence of only odd-numbered levels of O_2 rotational states makes it easier to assign the partially resolved rotational structures. The most interesting phenomenon is extremely high-energy transfer from translational to vibrational excitation in the backward direction, which could be explained involving charge transfer between proton and O_2 molecule and possibly complex formation in the inelastic collision process. The experimental results presented here provide us deep insight into this interesting inelastic scattering process.

EXPERIMENTAL METHOD

In this work, full quantum-state resolved inelastic scattering of high- n Rydberg H atom with O_2 was carried out by using HRTOF technique, which was pioneered by Welge and coworkers.^{27,28} The experimental apparatus used in this study has been described in detail elsewhere,^{17,25} and only a brief description is presented here. Molecular beams (HI and O_2) are generated by an adiabatic expansion through two parallel pulsed valves. The complete cooling of the O_2 beam would be obtained under the adiabatic expansion condition. Faubel et al.²⁹ has demonstrated that more than 93% of the O_2 molecules are in $j=1$, and $\sim 7\%$ of the molecules are in $j=3$. The H-atom beam is produced from HI photodissociation at 266 nm in the molecular beam using a Nd:YAG fourth harmonic laser output. There are two different photolysis channels relative to the two spin–orbit states of the iodine atom ($I_{3/2}$ and $I_{1/2}$), which give rise to two sharp peaks of H-atom velocity distribution (a fast component with the center peak at 17 470 m/s and a slow component with the center peak at 11 230 m/s). After traversing a distance of 25 mm (5 mm below the center of the O_2 molecular beam), the H atoms are excited to a high Rydberg level ($n=46$) directly by resonant two-photon excitation via the $H(2p)$ state using two excitation laser beams of 121.6 and 365.8 nm wavelengths.³⁰ Then, the H-RA crosses the O_2 molecular beam at 90° . The scattered H-RA travels a certain TOF distance before reaching the rotating multichannel plate (MCP) detector with a fine metal grid (grounded) in the front. After passing through the grid, the H-RA is immediately field-ionized by the electric field applied between the front plate of the Z-stack MCP detector and the fine metal grid and finally detected by the Z-stack MCP detector. In an effort to measure complete angular distribution by the rotating MCP detector in this experiment, a liquid nitrogen (LN_2)-cooled copper block is installed downstream of the HI molecular beam. This copper block could significantly eliminate the attenuation of the scattering signals in the forward directions ($(\theta_{lab} < -40^\circ)$) through absorbing the HI beam during scattering.²⁵

AUTHOR INFORMATION

Corresponding Author

*E-mail: kjyuan@dicp.ac.cn (K.Y.), xmyang@dicp.ac.cn (X.Y.).

Notes

The authors declare no competing financial interest.

ACKNOWLEDGMENTS

This work was supported by the National Natural Science Foundation of China (no. 21103185), the Chinese Academy of Sciences, and the Ministry of Science and Technology.

REFERENCES

- (1) Krstic, P. S.; Schultz, D. R. Elastic and Vibrationally Inelastic Slow Collisions: $\text{H} + \text{H}_2$, $\text{H}^+ + \text{H}_2$. *J. Phys. B: At., Mol. Opt. Phys.* **1999**, *32*, 2415–2431.
- (2) Kumar, T. J.; Kumar, S. Low-Energy Rotational Inelastic Collisions of $\text{H}^+ + \text{CO}$ System. *J. Chem. Phys.* **2012**, *136*, 044317.
- (3) Hege, U.; Linder, F. Vibrationally Inelastic Scattering of H^- Ions from H_2 , N_2 , O_2 and CO_2 . *Z. Phys. A* **1985**, *320*, 95–104.
- (4) Miller, W. H. The Semiclassical Nature of Atomic and Molecular Collisions. *Acc. Chem. Res.* **1971**, *4*, 161–167.
- (5) McBane, G. C.; Kable, S. H.; Houston, P. L.; Schatz, G. C. Collisional Excitation of CO by 2.3 eV H Atoms. *J. Chem. Phys.* **1991**, *94*, 1141–1149.
- (6) Chawla, G. K.; McBane, G. C.; Houston, P. L.; Schatz, G. C. State-Selective Studies of $\text{T} \rightarrow \text{R}, \text{V}$ Energy Transfer: The $\text{H} + \text{CO}$ System. *J. Chem. Phys.* **1988**, *88*, 5481–5488.
- (7) Kreutz, T. G.; Flynn, G. W. Analysis of Translational, Rotational, and Vibrational Energy Transfer in Collisions Between CO_2 and Hot Hydrogen Atoms: The Three-Dimensional “Breathing” Ellipsoid Model. *J. Chem. Phys.* **1990**, *93*, 452–456.
- (8) Wight, C. A.; Donaldson, D. J.; Leone, S. R. A Two-Laser Pulse-and-Probe Study of T-R, V Energy Transfer Collisions of $\text{H} + \text{NO}$ at 0.95 and 2.2 eV. *J. Chem. Phys.* **1985**, *83*, 660–667.
- (9) Goldberg, N. T.; Zhang, J. Y.; Koszinowski, K.; Bouakline, F.; Althorpe, S. C.; Zare, R. N. Vibrationally Inelastic $\text{H} + \text{D}_2$ Collisions are Forward-Scattered. *Proc. Natl. Acad. Sci. U.S.A.* **2008**, *105*, 18194–18199.
- (10) Greaves, S. J.; Wrede, E.; Goldberg, N. T.; Zhang, J. Y.; Miller, D. J.; Zare, R. N. Vibrational Excitation through Tug-of-War Inelastic Collisions. *Nature* **2008**, *454*, 88–91.
- (11) Udseth, H.; Giese, C. F.; Gentry, W. R. Rotational Excitation in the Small-Angle Scattering of Protons from Diatomic Molecules. *J. Chem. Phys.* **1974**, *60*, 3051–3056.
- (12) Krutein, J.; Linder, F. Measurements of Vibrational Excitation of N_2 , CO, and NO by Low Energy Proton Impact. *J. Chem. Phys.* **1979**, *71*, 599–604.
- (13) Gianturco, F. A.; Gierz, U.; Toennies, J. P. Anomalous Vibrational Excitation of O_2 in Collisions with Protons at 10 eV when Compared with N_2 , CO and NO. *J. Phys. B: At., Mol. Opt. Phys.* **1981**, *14*, 667–677.
- (14) Noll, M.; Toennies, J. P. Vibrational State Resolved Measurements of Differential Cross Sections for $\text{H}^+ + \text{O}_2$ Charge Transfer Collisions. *J. Chem. Phys.* **1986**, *85*, 3313–3325.
- (15) George, F.; Xavier, D.; Kumar, S. Ab Initio Adiabatic and Quasidiabatic Potential Energy Surfaces of Lowest Four Electronic States of the $\text{H}^+ + \text{O}_2$ System. *J. Chem. Phys.* **2010**, *133*, 164304.
- (16) Sizun, M.; Grimbert, D.; Sidis, V.; Baer, M. Vibrational State-to-State Calculations of $\text{H}^+ + \text{O}_2$ Charge Transfer Collisions. *J. Chem. Phys.* **1992**, *96*, 307–325.
- (17) Dai, D. X.; Wang, C. C.; Wu, G. R.; Harich, S. A.; Song, H.; Hayes, M.; Skodje, R. T.; Wang, X. Y.; Gerlich, D.; Yang, X. M. State-to-State Dynamics of High- n Rydberg H-Atom Scattering with D_2 . *Phys. Rev. Lett.* **2005**, *95*, 013201.
- (18) Wrede, E.; Schnieder, L.; Seekamp-Schnieder, K.; Niederjohann, B.; Welge, K. H. Reactive Scattering of Rydberg Atoms: $\text{H}^* + \text{D}_2 \rightarrow \text{HD} + \text{D}^*$. *Phys. Chem. Chem. Phys.* **2005**, *7*, 1577–1582.
- (19) Song, H.; Dai, D. X.; Wu, G. R.; Wang, C. C.; Harich, S. A.; Hayes, M. Y.; Wang, X. Y.; Gerlich, D.; Yang, X. M.; Skodje, R. T. Chemical Reaction Dynamics of Rydberg Atoms with Neutral Molecules: A Comparison of Molecular-Beam and Classical Trajectory Results for the $\text{H}(n) + \text{D}_2 \rightarrow \text{HD} + \text{D}(n')$ Reaction. *J. Chem. Phys.* **2005**, *123*, 074314.
- (20) Gerlich, D. Ph.D. Thesis, University of Freiburg, 1977.
- (21) Fermi, E. Sopra Lo Spostamento Per Pressione Delle Righe Elevate Delle Serie Spettrali. *Nuovo Cimento* **1934**, *11*, 157–166.
- (22) Stebbings, R. F.; Dunning, F. B. *Rydberg States of Atoms and Molecules*; Wiley: New York, 1983.
- (23) Lebedev, V. S.; Beigman, I. L. *Physics of Highly Excited Atoms and Ions*; Wiley: Berlin, 1998.
- (24) Strazisar, B. S.; Lin, C.; Davis, H. F. Vibrationally Inelastic Scattering of High- n Rydberg H Atoms from N_2 and O_2 . *Phys. Rev. Lett.* **2001**, *86*, 3997–4000.
- (25) Yu, S. R.; Yuan, K. J.; Song, H.; Xu, X.; Dai, D. X.; Zhang, D. H.; Yang, X. M. State-to-State Differential Cross-Sections for the Reactive Scattering of $\text{H}^*(n)$ with $o\text{-D}_2$. *Chem. Sci.* **2012**, *3*, 2839–2842.
- (26) Giese, C. F.; Gentry, W. R. Classical Trajectory Treatment of Inelastic Scattering in Collisions of H^+ with H_2 , HD, and D_2 . *Phys. Rev. A* **1974**, *10*, 2156–2175.
- (27) Schnieder, L.; Meier, W.; Wrede, E.; Welge, K. H.; Ashfold, M. N. R.; Western, C. M. Photodissociation Dynamics of H_2S at 121.6 nm and a Determination of the Potential Energy Function of $\text{SH}(\text{A}^2\Sigma^+)$. *J. Chem. Phys.* **1990**, *92*, 7027–7037.
- (28) Schnieder, L.; Seekamp-Rahn, K.; Wrede, E.; Welge, K. H. Experimental Determination of Quantum State Resolved Differential Cross Sections for the Hydrogen Exchange Reaction $\text{H} + \text{D}_2 \rightarrow \text{HD} + \text{D}$. *J. Chem. Phys.* **1997**, *107*, 6175–6195.
- (29) Faubel, M.; Kraft, G. Ar- O_2 Rotationally Inelastic Collisions. *J. Chem. Phys.* **1986**, *85*, 2671–2683.
- (30) Schnieder, L.; Seekamp-Rahn, K.; Borkowski, J.; Wrede, E.; Welge, K. H.; Aoiz, F. J.; Banares, L.; D’Mello, M. J.; Herrero, V. J.; Saez Rabanos, V.; Wyatt, R. E. Experimental Studies and Theoretical Predictions for the $\text{H} + \text{D}_2 \rightarrow \text{HD} + \text{D}$ Reaction. *Science* **1995**, *269*, 207–210.